Visualization of α9 acetylcholine receptor expression in hair cells of transgenic mice containing a modified bacterial artificial chromosome

Jian Zuo*†, Jason Treadaway†, Tyler W. Buckner†, and Bernd Fritzsch‡

†Department of Developmental Neurobiology, St. Jude Children's Research Hospital, Memphis, TN 38105; and ‡Department of Biomedical Sciences, Creighton University, Omaha, NE 68178

Communicated by Richard L. Sidman, Harvard Medical School, Southborough, MA, October 1, 1999 (received for review June 24, 1999)

The α9 acetylcholine receptor (α9 AChR) is specifically expressed in hair cells of the inner ear and is believed to be involved in synaptic transmission between efferent nerves and hair cells. Using a recently developed method, we modified a bacterial artificial chromosome containing the mouse α9 AChR gene with a reporter gene encoding green fluorescent protein (GFP) to generate transgenic mice. GFP expression in transgenic mice recapitulated the known temporal and spatial expression of α9 AChR. However, we observed previously unidentified dynamic changes in α9 AChR expression in cochlear and vestibular sensory epithelia during neonatal development. In the cochlea, inner hair cells persistently expressed high levels of α9 AChR in both the apical and middle turns, whereas both outer and inner hair cells displayed dynamic changes of α9 AChR expression in the basal turn. In the utricle, we observed high levels of α9 AChR expression in the striolar region during early neonatal development and high levels of α9 AChR in the extrastriolar region in adult mice. Further, simultaneous visualization of efferent innervation and α9 AChR expression showed that dynamic expression of α9 AChR in developing hair cells was independent of efferent contacts. We propose that α9 AChR expression in developing auditory and vestibular sensory epithelia correlates with maturation of hair cells and is hair-cell autonomous.

Hair cells of the inner ear are the mechanosensory transducers involved in hearing and balance (1). In mammals, hair cells are distributed in the cochlea and in five vestibular organs: the utricle, the saccule, and three semicircular canals. Much has been learned about inner ear development by using the targeted gene disruption strategy (2, 3). In contrast, our understanding of hair cell function has been hampered by the lack of effective means to express genes into hair cells *in vivo* (4). It is possible to use mouse embryonic stem cell technology to introduce the reporter gene at the locus of a hair cell-specific gene (5). However, it is difficult to express a reporter gene at a high level when the endogenous gene is expressed at a low level, therefore limiting the utility of this method (6). Alternatively, conventional transgenic technology has been successfully used in other neurons for such a purpose (7, 8). A previous attempt to express reporter genes in hair cells of transgenic mice, however, was unsatisfactory (9). This failure was probably because of the lack of proper regulatory elements in the promoter constructs used in generating transgenic mice. A strategy was recently developed to overcome the limitations of conventional transgenic methods (10). Bacterial artificial chromosome (BAC) was modified with a reporter gene by homologous recombination in bacteria, and the modified BAC was subsequently used to create transgenic mice that express the reporter gene in specific neurons. This methodology eliminates the need to analyze a large number of promoter constructs and transgenic lines, because the BAC clones, usually containing more than 100 kilobase (kb) genomic DNA surrounding the endogenous gene, likely include all the necessary regulatory elements (i.e., locus control region and enhancer) (11, 12). BAC clones should therefore be sufficient to express a reporter gene in a pattern identical to the endogenous gene. Green fluorescent protein (GFP) is an ideal reporter in mice, because it can be visualized *in vivo* with high sensitivity but without using any substrates, as required for the LacZ reporter (5). GFP can also be used for fluorescence-activated cell sorting, which has been successfully applied to other cell types (13). We report here our success in using this methodology to express GFP in hair cells in transgenic mice.

During the formation of the neuromuscular junction, initial expression of nicotinic acetylcholine receptors (AChR) in muscle cells is nerve independent, controlled by the differentiation program of muscle cells. On nerve arrival, AChRs in muscle cells undergo aggregation, up-regulation, and transformation into adult form that is likely nerve dependent (14). These dynamic changes of AChR expression in the formation of neuromuscular junction have been implicated, but not documented, in synaptic formation in other areas of the central nervous system and the peripheral nervous system. In the mammalian inner ear, for example, hair cells receive efferent innervation from the superior olivary complex, located in the brainstem (15). Given that efferent neurons are developmentally related to facial branchial motoneurons (16), it is possible that the interaction between hair cells and efferents recapitulates the formation of the neuromuscular junction. Because acetylcholine is one of the principal neurotransmitters for signaling between efferent fibers and hair cells (17), it has been hypothesized that AChR plays a role in synapse formation between hair cells and efferent termini. Recently, a nicotinic acetylcholine receptor, α9 AChR, was identified (18). *In situ* hybridization studies demonstrated that α9 AChR is specifically expressed in hair cells in the developing and adult cochlea and in the vestibular inner ear, whereas it is likely no other subunits of AChRs are expressed in hair cells (18–24). It has therefore been proposed that the α9 AChR is involved in cholinergic efferent synaptic transmission to hair cells. Consistent with this hypothesis, the α9 AChR knockout mice display abnormalities in morphology of efferent termini innervating most outer hair cells (OHCs); functionally, they also fail to show the normal suppression of cochlear responses during efferent fiber stimulation (25). However, it remains unclear how closely α9 AChR expression correlates with efferent innervation, and whether α9 AChR expression displays dynamic changes like the neuromuscular junction.

Abbreviations: AChR, acetylcholine receptor; GFP, green fluorescent protein; BAC, bacterial artificial chromosome; E*n*, embryonic day *n*; P*n*, postembryonic day *n*; IHC, inner hair cells; OHC, outer hair cells; IRES, internal ribosome entry site; FISH, fluorescence *in situ* hybridization; RT-PCR: reverse transcriptase—PCR; DiI, 1,1′-dioctadecyl-3,3,3′,3′-tetramethylindocarbocyanine; kb, kilobase.

*To whom reprint requests should be addressed at: Department of Developmental Neurobiology, St. Jude Children's Research Hospital, 332 North Lauderdale Street, Memphis, TN 38105. E-mail: jian.zuo@stjude.org.

The publication costs of this article were defrayed in part by page charge payment. This article must therefore be hereby marked "*advertisement*" in accordance with 18 U.S.C. §1734 solely to indicate this fact.

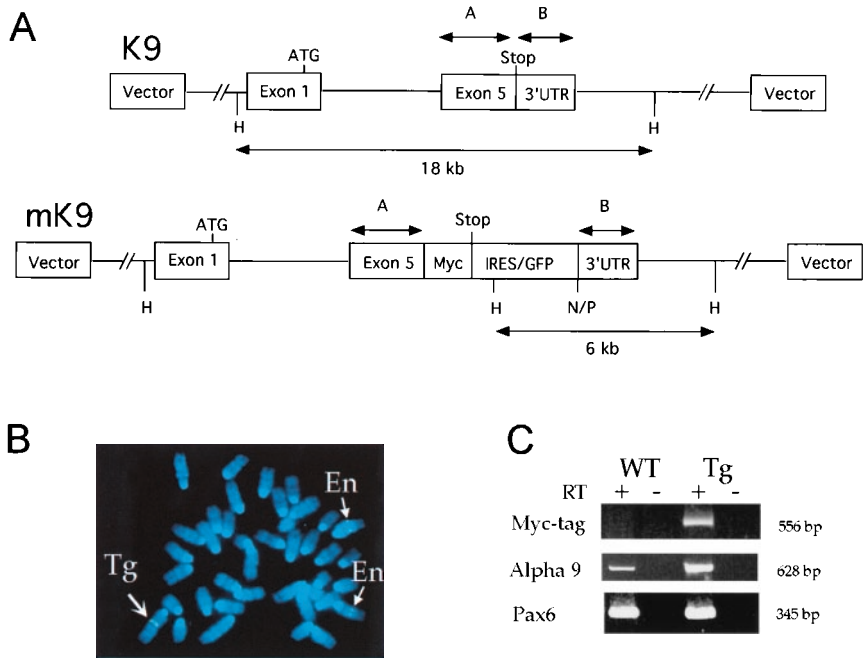

Fig. 1. (*A*) Site-directed mutagenesis of a BAC containing the mouse α9 AChR gene. In 13K9 (K9, 140 kb), a myc-tag was inserted before the stop codon in exon 5 of the α9 AChR gene, and an IRES/GFP cassette (1.3 kb) was inserted after the stop codon. Two homologous fragments, A (541 bp) and B (321 bp), which contain the coding portion and the 3′untranslated region (3′UTR) of exon 5, respectively, were used for modification of K9. The IRES/GFP cassette in modified K9 (mK9) contains additional *Not*I (N), *Pme*I (P), and *Hin*dIII (H) sites. Whereas exons 1–4 are intact, only exon 1 with the ATG start codon is depicted, for simplicity. (*B*) FISH analysis of metaphase embryonic fibroblast cells from transgenic mice by using K9 BAC DNA. Blue color (4,6-diamidino-2-phenylindole) staining represents each of 40 metaphase chromosomes. K9 BAC DNA hybridized (in green color) to two endogenous α9 AChR loci on two chromosomes 4 (thin arrows and En), and a third transgenic integration locus on chromosome 1 (thick arrow and Tg). At each locus of the three chromosomes, two sister chromatids gave a pair of identical hybridization signals. (*C*) RT-PCR analysis of α9 AChR endogenous and fusion transcripts in nasal epithelia of wild-type (WT) and transgenic (Tg) mice. Identical amounts of RNA templates were used in each PCR reaction. Presence (+) and absence (−) of RT were used as controls for each RNA sample. Three pairs of primers [labeled as Myc-tag, α9, and Pax6 (*Left*)] were used for each RNA sample in 35-cycle PCR reactions. PCR products were analyzed in 10% acrylamide gels, and sizes of these products were indicated (*Right*). Primers used here were described in the text.

Because α9 AChR is an excellent molecular marker specific for hair cells in the inner ear, we utilized the BAC modification strategy and generated transgenic mice that express GFP in a pattern identical to the known pattern of the endogenous α9 AChR expression revealed by *in situ* hybridization. Moreover, we observed previously unidentified dynamic changes in α9 AChR expression in cochlear and vestibular sensory epithelia during neonatal development that are inconsistent with the hypothesized role of αq AChR in synapse formation. Simultaneous visualization of efferent innervation and α9 AChR expression *in vivo* showed that α9 AChR expression in developing hair cells is independent of efferent innervation.

Materials and Methods

Modification of BAC Clones That Contain α9 AChR Gene. We screened the mouse BAC library (Catalogue no. 96050, Research Genetics, Huntsville, AL) in 129SV background with a cDNA clone encoding the rat α9 nAChR gene (kindly provided by S. F. Heinemann and D. E. Vetter, Salk Institute, San Diego, CA). Two BAC clones, 13K9 and 31O24, were isolated and characterized by Southern blot analysis and pulsed-field gel electrophoresis.

We inserted a reporter gene into the α9 AChR gene locus within the 13K9 BAC clone. To avoid extensive alteration of the coding region of the transgene, we inserted only one copy of the sequence encoding the c-myc tag (MEQKLISEEDLNE) at the 3′ end of the coding region before the stop codon in exon 5. An internal ribosome entry site (IRES) and a gene encoding the enhanced GFP cassette (kindly provided by N. Heintz and X. W. Yang, Rockefeller University, New York) were inserted after the stop codon in exon 5 (Fig. 1*A*). Two homologous fragments from exon 5 were amplified by PCR by using high-fidelity *Taq* polymerase and the following oligonucleotide primers: α9A1 (5′-ATCCGGAATTCCGGAAAATACTACATAGCTACC--3′) and α9A2 (5′-ATCCGGAATTCTATTCATTCAAGTCC-TCTTCAGAAATGAGCTTTTGCTCCATATCTGCTC-3′) were used to generate fragment A of 541 bp; α9B1 (5′-GACT-AGTCTAGACAGGAAAGAGGAGTGGGCTGG-3′) and α9B3 (5′-GGCTAGTCTAGACTAGGAATACACTGTGCTT-TGTTG-3′) were used to generate fragment B of 327 bp. We followed procedures to modify BACs, as previously described (10). Several independent resolved BAC clones were characterized by Southern blot analysis and pulsed-field gel electrophoresis. One clone, mK9–42, was analyzed by PCR by using a combination of primers: α9A1, α9A3 (5′-GCCAAATGTCT-CAAGGACCAC-3′), IRES-1 (5′-CTCGTCAAGAAGACAG-GGCCAGG-3′), IRES-2 (5′-TTTAACCTCGACTAAACAC-AC-3′), EGFP1–1 (5′-CCGGGATCACTCTCGGCATGGAC--3′), and α9B3. PCR products were sequenced to confirm their identity.

Genotyping of Transgenic Mice. Genotypes of the founder offspring were determined by using PCR with the following primers: BAC-1F (5′-TAACTATGCGGCATCAGAGC-3′) and BAC-1R (5′-GCCTGCAGGTCGACTCTAGAG-3′) with an expected ≈330 bp PCR fragment; EGFP1–1 and α9B3, with an expected ≈430 bp PCR fragment. Southern blot analysis of genomic DNA from transgenic mice was performed by using standard protocols.

Fluorescence *in situ* hybridization (FISH) analysis of trans-

genic mice was performed as described (26). Mouse embryonic fibroblast cell lines were made from individual embryonic day 13 (E13) embryos of a heterozygous transgenic female mouse. Metaphase chromosomes from these lines were hybridized with digoxigenin-11-dUTP-labeled probe derived from the entire 13K9 BAC DNA (Qiagen; Boehringer Mannheim). The metaphase chromosomes were stained with 4,6-diamidino-2-phenylindole and analyzed. Total fluorescence intensity of signal was measured for each locus of the same cell, and its intensity relative to that of the endogenous signal was calculated (26). The position of the transgene insertion locus was determined by conducting fractional length measurements of metaphase chromosomes.

RNA was isolated from nasal epithelia of three wild-type and three transgenic (a combination of heterozygous and homozygous) adult mice following standard protocols (Trizol, GIBCO/BRL). Reverse transcriptase–PCR (RT-PCR) was performed following standard protocols (Sensiscript RT kit, Qiagen). Twenty to thirty-five cycles were used for semiquantitative PCR analysis. Myc-tag specific primers were: A9A2Myc-SP6 (5′-ATTTAGGTGACACTATAGAACCTCTTCAGAAATGAGCTTTTG-5′); A9A1-T7 (5′-TAATACGACTCACTATAGGAGGAAAAATACTACATAGCTACC-3′). α9 specific primers were: A9E4-F784 (5′-CTAATGGTGGCAGAGATCATG-3′); A9A2-SP6 (5′-ATTTAGGTGACACTATAGAAATCTGCTCTTGCTATGATCAAG-3′). Pax6 specific primers were: Pax6-F811 (5′-CGACTTCAGCTGAAGCGGAA-3′); Pax6-R1160 (5′-TCTGTTCGGCCCAACATGGA-3′).

Immunostaining and Epifluorescence of Hair Cells and 1,1′-Dioctadecyl-3,3,3′,3′-Tetramethylindocarbocyanine (DiI) Labeling of Efferents. Antibodies used in this study include monoclonal antibody 9E10 against myc-tag from Babco (Richmond, CA), anti-myc monoclonal antibody from Invitrogen, anti-Myc Tag rabbit polyclonal IgG from Upstate Biotechnology (Lake Placid, NY), myoVI- and myoVIIa-specific antibodies (gifts from T. Hasson, University of California, San Diego, CA), purified rabbit anti-GluR δ½, and rabbit anti-Calretinin polyclonal antibodies (Chemicon). Immunostaining procedures were followed as recommended by the manufacturers.

DiI labeling of the efferents was as described (15). For GFP and DiI detection, we recorded epifluorescence by using a cooled CCD camera set to average 25 sweeps of each slide to increase the signal-to-noise ratio. We also used a polyclonal antibody (CLONTECH) specific for GFP to detect GFP expression using horseradish peroxidase-diaminobenzamidine reaction. Whole mounts of the inner-ear cochleas were viewed and were subsequently embedded in epoxy resin for semithick and ultrathin sections to verify cell-specific localization (data not shown).

Results

Transgenic Mice Using Modified BAC. We isolated a 140-kb mouse BAC clone 13K9 (K9) that contained the α9 AChR gene. To introduce a reporter gene at the α9 AChR gene locus in the BAC K9, we inserted a single copy of the c-myc epitope tag before the stop codon, which was adjacent to a reporter gene cassette containing IRES/GFP (Fig. 1*A*). Detailed restriction analysis by pulsed-field gel electrophoresis indicated that the modified BAC clone (mK9) did not contain any detectable rearrangement except for the IRES/GFP insertion (data not shown). By using a *Not*I site and a *Pme*I site at the end of the IRES/GFP cassette, we showed that mK9 contained at least 45 kb of the genomic fragment upstream of the stop codon of the α9 AChR gene. Further, the first exon, which contained the 5′untranslated region and the initiation ATG codon, and the last exon, which contained the stop codon, were mapped to the same 18-kb *Hin*dIII fragment (Fig. 1*A*; data not shown). Therefore, the modified BAC clone contained at least 27 kb of genomic DNA upstream from the initiation codon. Transgenic mice containing the modified BAC were expected to express mRNA fusion transcripts encoding both myc-tagged α9 AChR and GFP. The portion of the transcript encoding the myc-tagged α9 AChR was expected to be translated by the cap-mediated mechanism; the portion encoding GFP was expected to be translated by the IRES-mediated mechanism (27).

Linearized mK9 DNA was purified by using the CsCl/Sepharose CL4b method (10) and injected at a concentration of 1.4 μg/ml into pronuclei of FVB/NJ female mice. Southern hybridization and PCR analyses showed that one of the offspring (Tg8) was positive for the transgene (data not shown). The insertion of the IRES/GFP cassette into the BAC disrupted the endogenous 18-kb *Hin*dIII fragment and resulted in a 6-kb *Hin*dIII fragment that was detected by hybridization with fragment B containing the 3′untranslated region (data not shown). Additional hybridization by using probes representing the BAC vector arm, the first exon of the α9 AChR gene, the IRES/GFP cassette, and the junction between the GFP gene and fragment B, indicated that the intact mK9 DNA was present in the genomic DNA of Tg8 (data not shown). These results were confirmed by sequencing the PCR products.

To estimate the copy number of the transgene and to determine the transgene insertion site in the genome, we performed FISH analysis on metaphase chromosomes of mouse embryonic fibroblast (MEF) (early passage) cell lines derived from offspring of a transgenic female at E13 (Fig. 1*B*). The K9 BAC DNA hybridized to an endogenous locus on chromosome 5, consistent with previous mapping results (www.informatics.jax.org). An additional stronger signal was detected on chromosome 1. Because MEF metaphase cells from wild-type embryos did not contain this additional signal, it thus represented the transgenic BAC insertion locus. We measured the total fluorescence intensity of the transgenic signal (26) relative to that of the endogenous signal (one copy) of each cell: the ratio between the two was 5.0 ± 2.8 (mean ± SD; $n = 20$). Therefore, the copy number of the BAC transgene is about 5. In addition, we determined that the BAC transgene integration site is in cytogenetic band 1C4–1C5 or ≈36% of the entire length of chromosome 1 from the heterochromatin–euchromatin boundary near the centromere to the telomere.

To estimate the relative ratio of the α9 AChR fusion transcript and the endogenous transcript in transgenic mice, we performed RT-PCR analysis of RNA samples in wild-type and transgenic mice. Because the α9 AChR gene is expressed in the nasal epithelium, we isolated RNA from nasal epithelia of adult mice and performed RT-PCR using three sets of primers: one specific for the myc-tag portion of the α9 AChR fusion transcript, another specific for both α9 AChR endogenous and fusion transcripts, the third specific for the Pax6 gene as a control (Fig. 1*C*). The presence of a product in transgenic mice by using myc-tag specific primer set demonstrated that the myc-tag is present in the α9 AChR fusion transcript. Semiquantitative analysis of products from both wild-type and transgenic mice by using α9 AChR-specific primers showed that the fusion transcript is ≈8 times more abundant than the endogenous transcript (Fig. 1*C*). To assess the myc-tagged α9 AChR fusion protein, we performed immunohistochemistry and Western blot analyses of cochleas from wild-type and transgenic mice at postembryonic day (P) 0, P2, P5, P8, and P13. None of three antibodies against myc-tag resulted in a specific signal in hair cells as expected. Further characterization of α9 AChR protein distribution in wild-type and transgenic mice is in progress (23).

The transgenic founder female mouse was normal in size and was fertile. Both male and female offspring were fertile and were maintained in the original FVB/NJ strain background. Genotypes of the progeny were determined by using PCR methods (data not shown). The founder and the transgenic progeny displayed normal startle responses and vestibular functions. Further, hair cells of transgenic mice express other hair-cell molecular markers such as MyoVIIa, MyoVI, GluR δ1, and Calretinin (data not shown).

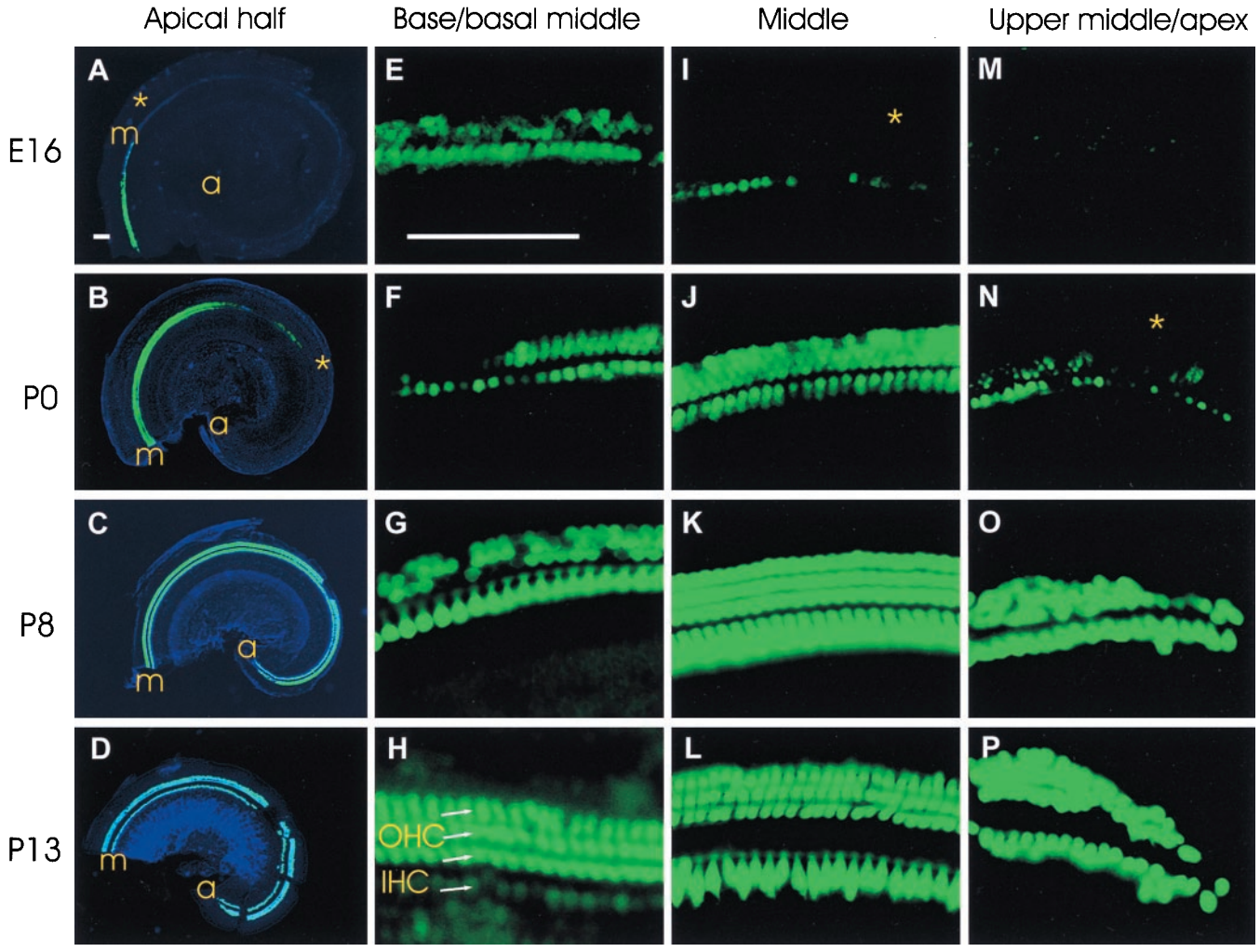

Fig. 2. Developmental pattern of GFP expression in hair cells of cochlea in transgenic mice from E16 to P13. (*A–D*) Flat-mounted cochlea of the apical half of the cochlea at E16, P0, P8, and P13, respectively. GFP epifluorescence (green) is superimposed on the cochlear outline visualized by DIC (blue). Gaps at P8 and P13 are preparation artifacts. a, apex; m, middle turn. (*E–H*) Immunodetection of GFP on flat mounts of the base/basal part of the middle turns of the cochlea at E16, P0, P8, and P120 (adult), respectively. (*I–L*) GFP immunodetection on flat mounts of the middle turns of the cochlea at E16, P0, P8, and P13, respectively. (*M–P*) Immunodetection of GFP on flat mounts of the upper middle turns at E16, P0, and the apical turns at P8 and P13, respectively. Stars in *A* and *I*, *B* and *N* correspond to similar positions. *A–D* are at the same magnification, and *E–P* are at the same magnification. Bars = 100 μm.

Detailed analysis of the auditory responses of transgenic mice is in progress.

Expression of GFP in Hair Cells. Expression of GFP in the developing inner ear of the transgenic progeny was analyzed. GFP was highly expressed in hair cells of the cochlea, saccule, utricle, and sensory epithelia of the semicircular canal. GFP was not expressed in supporting cells in the inner ear (data not shown). GFP appeared to be evenly distributed in the cytoplasm and nuclei of hair cells (data not shown). The minimal concentration of cytosolic GFP that can be detected by epifluorescence is 1 μM (28); we estimate that the concentration of GFP in most hair cells of transgenic mice was at least 10 μM (data using fluorescence-activated cell sorting; not shown). By using immunocytochemistry, low levels of GFP expression were found in spiral ganglia at P8 and adult but not at P5 or before (data not shown). In addition, large amounts of GFP were expressed in pars tuberalis of the hypophyseal gland, neurons in nasal epithelium, sternohyoid muscle, intrinsic musculature of the tongue, and blood cells in capillaries on E16 (data not shown). These observations are consistent with previous *in situ* hybridization studies (18–24). No GFP expression was detected in any other areas of the central nervous system that we examined.

No GFP expression was detected in inner ear at E13. At E16, all hair cells of the vestibular part of the inner ear were GFP positive, and only a few hair cells in cochlea started to express GFP. The pattern of GFP expression in the cochlea changed dynamically from E16 to adulthood in both longitudinal (base to apex) and radial [inner hair cells (IHCs) to OHCs] directions (Fig. 2). At E16, GFP was first detected in many IHCs and some OHCs of the basal turn, as well as in IHCs of the middle turn. At P0, GFP was detected in hair cells near the apex. By P8, most cochlear hair cells were GFP positive. In the radial direction, GFP expression in IHCs always preceded expression in OHCs (Fig. 2 *A*, *B*, *I*, and *N*). In OHCs at the base, there was a drastic reduction in the intensity of the GFP signal between P0 and P8 (Fig. 2 *F* and *G*). This reduction was followed by an increase in GFP signal intensity in OHCs and by a concurrent decrease in GFP signal intensity in IHCs between P8 and P13 to adulthood (Fig. 2 *G* and *H*). However, in the middle turn, GFP signal intensity remained strong in both OHCs and IHCs between P0 and P13 to adulthood (Fig. 2*J–L*). From P8 to P13, both OHCs and IHCs at the apex highly expressed GFP (Fig. 2 *O* and *P*). These differences in GFP expression during development were reproduced in at least two different litters and have been confirmed

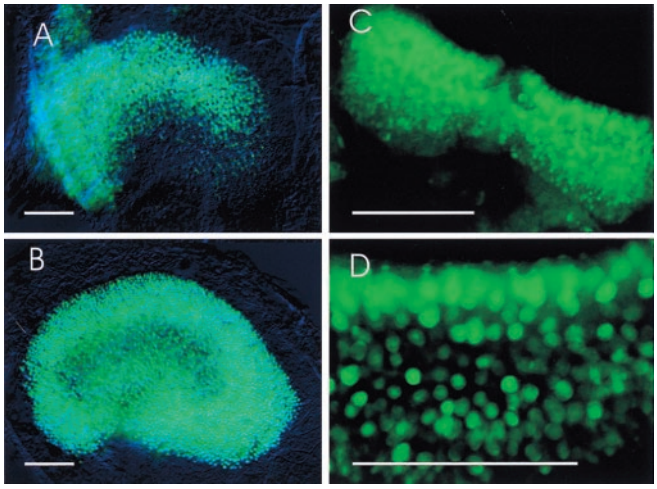

Fig. 3. Developmental pattern of GFP expression in hair cells of the utricle and semicircular canal. (*A* and *B*) GFP immunodetection on flat mounts of the utricle at P2 and P120, respectively. (*C* and *D*) GFP immunodetection on flat mounts of the semicircular canal at P2 and P8, respectively. Bars = 100 μm.

by staining flat-mounted radial sections of the cochlea (data not shown).

We also observed a dynamic pattern of GFP expression in the inner-ear gravistatic sensory epithelia, the utricle, and the saccule in our transgenic line (Fig. 3). GFP expression was first detected in these vestibular sensory epithelia at E16 (data not shown). Expression was up-regulated in the striolar region at P2 (Fig. 3*A*). Down-regulation of GFP expression in the striolar region and up-regulation of expression in the extrastriolar region occurred at P13 (data not shown); the higher level of GFP expression in the extrastriola persisted into adulthood (Fig. 3*B*). In contrast, the gradient of GFP expression throughout the semicircular sensory epithelia remains constant during development (Fig. 3 *C* and *D*). Moreover, GFP is expressed by both type I and II hair cells in vestibular sensory epithelia (data not shown). These findings are consistent with those of *in situ* hybridization studies in chickens and rats (19, 29).

Another independent transgenic founder (Tg13) had a low copy number of the transgene (data not shown), and it did not transmit through the germline. We analyzed only the founder mouse at P180, and it displayed similar GFP expression in hair cells as in Tg8 but at a lower level (data not shown). Therefore, we concluded that GFP expression recapitulates the temporal and spatial expression patterns of the endogenous a9 AchR in these transgenic lines.

Simultaneous Visualization of Efferents and α9 AChR. To correlate efferent fiber innervation and the expression of α9 AChR in hair-cell development, we labeled the superior olivary nuclei of the transgenic mice with a red fluorescent dye, DiI (15), and visualized simultaneously the efferent innervation and GFP/α9 AChR expression before (Fig. 4), during, and after synaptogenesis. Surprisingly, we found that efferent fibers and α9 AChR expression do not completely correlate in all these developmental stages.

At E16, hair cells at the basal middle turn of the cochlea already expressed α9 AChR transcript a few days before efferent fibers contacted a few IHCs at the basal middle turn (Fig. 4), because the first synapses form with IHCs in the basal middle turn of the cochlea at P2 (30). In contrast, efferent fibers reach the IHCs of the apex at E16, several days before any α9 AChR transcript was detected (Fig. 2 *A* and *M*; Fig. 4*C*). Further, large amounts of α9 AChR transcript were expressed in OHCs at the middle turn at P0, a time when very few efferent fibers reached these OHCs (Fig. 2 *B* and *J*; data not shown). These data suggest that the initial regulation of α9

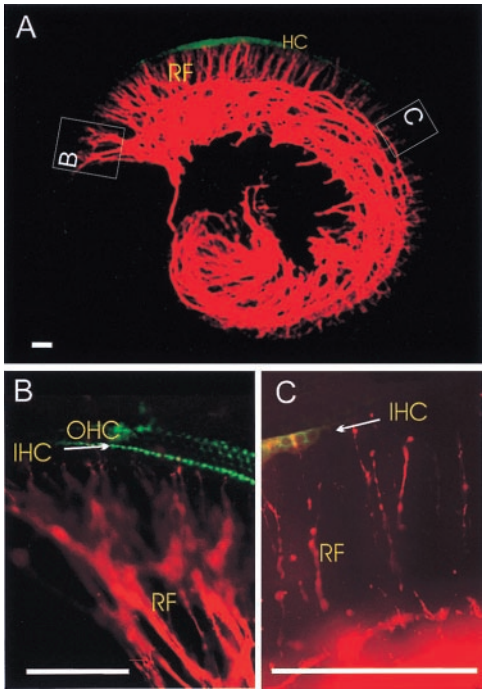

Fig. 4. Simultaneous visualization of GFP epifluorescence (green) and efferent fibers labeled with DiI (red) from the brainstem to the cochlea in a transgenic mouse at E16. (*A*) The entire cochlea. (*B*) The basal part of the basal turn. (*C*) The middle part of the middle turn. RF, radial fibers; IHC, inner hair cells; OHC, outer hair cells. Bars = 100 μm.

AChR expression is independent of the physical proximity of efferent innervation.

As previously noted (20), there was some correlation between the down-regulation of α9 AChR expression in IHCs in the basal turn after P8 (Fig. 2 *G* and *H*) and the shift of efferent terminals from IHCs to OHCs after P8 (30). However, OHCs of the basal turns show down-regulation of α9 AChR expression before P8 (Fig. 2 *F* and *G*). Further, OHCs of the apex did not undergo such changes (Fig. 2 *N* and *O*). Thus, α9 AChR expression does not fully correlate with the known dynamics of efferent innervation during synaptogenesis.

In the adult cochlea, α9 AChR was expressed in all OHCs and in most IHCs (Fig. 2*H*; data not shown), largely consistent with the known cholinergic efferent fibers distribution to the OHCs (31). However, α9 AChR was highly expressed in the IHCs and OHCs of the upper middle and apical turn (Fig. 2*P*), an area that receives predominantly γ-aminobutyric acid (GABA)ergic efferent innervation (32). These data suggest that in the adult cochlea, cholinergic efferent innervation correlates only partially with α9 AChR expression.

In the utricle of mice, most type I hair cells lack efferent innervation (33); it is predominantly type II hair cells that receive efferent innervation (34, 35). Recent data show that both types of hair cells are present in the striola and the extrastriola, and that there are more type I hair cells in the extrastriola than in the striola of the inner ear of the neonatal and adult mice (35). Therefore, the dynamic changes of α9 AChR expression in the utricle also do not correlate with the pattern of efferent innervation or the distribution of type I and II hair cells.

Discussion

GFP expression in our transgenic mice recapitulates cell-type specificity and developmental patterns of α9 AChR expression previously revealed by *in situ* hybridization (18–24). We observed both the longitudinal and radial gradients of GFP expression during

cochlear development that have been demonstrated in several reports on the α9 AChR expression (19, 20). On the basis of these results, we concluded that the modified BAC clone (mK9) contains all the necessary elements that control the specific expression of α9 AChR. We not only recapitulated the endogenous pattern but also amplified the signal of the α9 AChR transcript, because the copy number of the BAC transgene is $\approx$5, and the fusion transcript is several-fold more abundant than the endogenous transcript. In this preliminary study, we failed to detect myc-tag signal in cochlea of transgenic mice by either Western blot analysis or immunohistochemistry using three different myc-tag antibodies. This failure could be explained in part by the speculation that the short C terminus of α9 AChR may be buried within transmembrane domain IV. Alternatively, it is known that six or more copies of myc-tag would be beneficial for immunodetection by using these myc-tag antibodies. Nevertheless, it would be interesting to further investigate the α9 AChR protein distribution in the developing inner ear of transgenic mice by raising antibodies specifically against α9 AChR protein. Because the morphology of hair cells in transgenic mice appeared to be normal, hair cells express four other molecular markers, and the mice displayed normal startle responses, we therefore believed that the expression of the transgene in hair cells did not disturb hair-cell development and function at a detectable level. Our transgenic mice thus provide an invaluable resource for the hearing research community. These mice could be crossed to other mutant mouse strains to visualize the morphological development of hair cells *in vivo*. Further manipulation of mK9 BAC would enable us to introduce any exogenous genes specifically into hair cells, and the functions of these genes could thus be assayed *in vivo*. Moreover, hair cell-specific conditional knockout mouse strains could be created by further modifying our mK9 BAC. Individual hair cells could be sorted by using fluorescence-activated cell sorting for construction of hair cell-specific cDNA libraries.

Our results cannot be reconciled with a model in which efferent fibers regulate α9 AChR expression in direct physical proximity but suggest that intrinsic epithelia-derived signals may be responsible for α9 AChR regulation. Nerve-independent hair cell differentiation has been suggested previously by results of studies of organotypic cultures (35) and analyses of neurotrophin mouse mutants (36); we provide direct *in vivo* evidence supporting such a contention. Our data show that the pattern of α9 AChR expression is consistent with the progression of maturation of the inner ear. Starting on E15, hair-cell maturation spirals from the midbasal turns to both the apical and basal turns in cochlea (30, 37); this pattern along the cochlear partition corresponds to the distribution of α9 AChR-expressing cells that we observed at E16. IHCs generally mature before OHCs, consistent with the chronological order of α9 AChR expression in IHCs and OHCs. In developing utricles, hair cells in striola appear to be born and to differentiate earlier than those in extrastriola (35). It is thus likely that expression of α9 AChR is an intrinsic characteristic of hair cells, and that it is regulated by factors that also direct the maturation of hair cells.

It will now be interesting to determine whether the pattern and timing of α9 AChR expression seen *in vivo* is the same as that seen in both cochlear and vestibular sensory epithelia in organotypic cultures in which there is no efferent innervation (35) and in mutant mice lacking efferent innervation (36). The role of α9 AChR in the development of the cochlea remains unclear. Interestingly, it was recently reported that in addition to its nicotinic and muscarinic properties, α9 AChR also shares pharmacological properties with γ-aminobutyric acid $(GABA)_a$, 5-HT_3, and glycine receptors (38). This could partially explain our observation of the high level of α9 AChR expression in the apical turns, where there is predominantly GABAergic efferent innervation in adults. Findings in this study and others (18, 19) demonstrate that α9 AChR is expressed in nonneuronal tissues such as blood and muscle, suggesting that it may function in processes other than neurotransmission.

We thank X. W. Yang and N. Heintz for discussion and reagents for BAC modification; M. Valentine and V. Valentine for FISH analysis; C. Miller and M. Christensen for technical assistance; L. Li for pronuclear injection; A. J. Hudspeth for advice; S. F. Heinemann and D. E. Vetter for rat α9 AChR clone; T. Hasson for anti-MyoVIIa and MyoVI antibodies; and T. Curran, P. Fuchs, P. Gillespie, M. C. Liberman, S. Magdaleno, J. Morgan, N. Segil, D. Simmons, and R. Smeyne for comments on the manuscript. This work was supported in part by National Institutes of Health (NIH) Cancer Center Support CORE grant CA21765, NIH/National Cancer Institute Cancer Training Grant 5 R25 CA23944; by the American Lebanese Syrian Associated Charities (ALSAC); by a Research Grant No. 5-FY98-0725 from the March of Dimes Birth Defects Foundation (J.Z.); and by National Institute on Deafness and Other Communication Disorders grant DC00215-14A1 (B.F.).

1. Hudspeth, A. J. (1989) *Nature (London)* **341,** 397–404.
2. Fekete, D. M. (1999) *Trends Neurosci.* **22,** 263–269.
3. Fritzsch, B., Pirvola, U. & Ylikoski, J. (1999) *Cell Tissue Res.* **295,** 369–382.
4. Holt, J. R., Johns, D. C., Wang, S., Chen, Z. Y., Dunn, R. J., Marban, E. & Corey, D. P. (1999) *J. Neurophysiol.* **81,** 1881–1888.
5. Bermingham, N. A., Hassan, B. A., Price, S. D., Vollrath, M. A., Ben-Arie, N., Eatock, R. A., Bellen, H. J., Lysakowski, A. & Zoghbi, H. Y. (1999) *Science* **284,** 1837–1841.
6. Ma, Q., Chen, Z., del Barco Barrantes, I., de la Pompa, J. L. & Anderson, D. J. (1998) *Neuron* **20,** 469–482.
7. Smeyne, R. J., Oberdick, J., Schilling, K., Berrebi, A. S., Mugnaini, E. & Morgan, J. I. (1991) *Science* **254,** 719–721.
8. Tsien, J. Z., Chen, D. F., Gerber, D., Tom, C., Mercer, E. H., Anderson, D. J., Mayford, M., Kandel, E. R. & Tonegawa, S. (1996) *Cell* **87,** 1317–1326.
9. Xiang, M., Zhou, L. & Nathans, J. (1996) *Vis. Neurosci.* **13,** 955–962.
10. Yang, X. W., Model, P. & Heintz, N. (1997) *Nat. Biotechnol.* **15,** 859–865.
11. Grosveld, F., van Assendelft, G. B., Greaves, D. R. & Kollias, G. (1987) *Cell* **51,** 975–985.
12. Tuan, D. Y., Solomon, W. B., London, I. M. & Lee, D. P. (1989) *Proc. Natl. Acad. Sci. USA* **86,** 2554–2558.
13. Amrein, H. & Axel, R. (1997) *Cell* **88,** 459–469.
14. Sanes, J. R. & Lichtman, J. W. (1999) *Annu. Rev. Neurosci.* **22,** 389–442.
15. Fritzsch, B. & Nichols, D. H. (1993) *Hear. Res.* **65,** 51–60.
16. Bruce, L. L., Kingsley, J., Nichols, D. H. & Fritzsch, B. (1997) *Int. J Dev. Neurosci.* **15,** 671–692.
17. Eybalin, M. (1993) *Physiol. Rev.* **73,** 309–373.
18. Elgoyhen, A. B., Johnson, D. S., Boulter, J., Vetter, D. E. & Heinemann, S. (1994) *Cell* **79,** 705–715.
19. Luo, L., Bennett, T., Jung, H. H. & Ryan, A. F. (1998) *J. Comp. Neurol.* **393,** 320–331.
20. Simmons, D. D. & Morley, B. J. (1998) *Mol. Brain Res.* **56,** 287–292.
21. Hiel, H., Elgoyhen, A. B., Drescher, D. G. & Morley, B. J. (1996) *Brain Res.* **738,** 347–352.
22. Anderson, A. D., Troyanovskaya, M. & Wackym, P. A. (1997) *Brain Res.* **778,** 409–413.
23. Park, H. J., Niedzielski, A. S. & Wenthold, R. J. (1997) *Hear. Res.* **112,** 95–105.
24. Glowatzki, E., Wild, K., Brandle, U., Fakler, G., Fakler, B., Zenner, H. P. & Ruppersberg, J. P. (1995) *Proc. R. Soc. London Ser. B* **262,** 141–147.
25. Vetter, D. E., Liberman, M. C., Mann, J., Barhanin, J., Boulter, J., Brown, M. C., Saffiote-Kolman, J., Heinemann, S. F. & Elgoyhen, A. B. (1999) *Neuron* **23,** 93–103.
26. Poon, S. S., Martens, U. M., Ward, R. K. & Lansdorp, P. M. (1999) *Cytometry* **36,** 267–278.
27. Mountford, P. S. & Smith, A. G. (1995) *Trends Genet.* **11,** 179–184.
28. Zlokarnik, G., Negulescu, P. A., Knapp, T. E., Mere, L., Burres, N., Feng, L., Whitney, M., Roemer, K. & Tsien, R. Y. (1998) *Science* **279,** 84–88.
29. Lustig, L. R., Hiel, H. & Fuchs, P. A. (1999) *J. Vestibular Res.* **9,** 359–367.
30. Pujol, R., Lavigne-Rebillard, M. & Lenoir, M. (1998) *Development of Sensory and Neural Structures in the Mammalian Cochlea* (Springer, New York).
31. Vetter, D. E., Adams, J. C. & Mugnaini, E. (1991) *Synapse* **7,** 21–43.
32. Sobkowicz, H. M. (1992) in *Development of Auditory and Vestibular Systems 2*, ed. Romand, R. (Elsevier, Amsterdam), pp. 59–100.
33. Wackym, P. A., Popper, P., Ward, P. H. & Micevych, P. E. (1991) *Otolaryngology Head Neck Surg.* **105,** 493–510.
34. Lysakowski, A. & Goldberg, J. M. (1997) *J. Comp. Neurol.* **389,** 419–443.
35. Rusch, A., Lysakowski, A. & Eatock, R. A. (1998) *J. Neurosci.* **18,** 7487–7501.
36. Fritzsch, B., Silos-Santiago, I., Bianchi, L. & Farinas, I. (1997) *Semin. Cell Dev. Biol.* **8,** 277–284.
37. Chen, P. & Segil, N. (1999) *Development (Cambridge, U.K.)* **126,** 1581–1590.
38. Rothlin, C. V., Katz, E., Verbitsky, M. & Elgoyhen, A. B. (1999) *Mol. Pharmacol.* **55,** 248–254.